J Fusion Energ (2015) 34:140–147
DOI 10.1007/s10894-014-9773-7

ORIGINAL RESEARCH

Theoretical Predictions of Excitation Functions of Neutron-Induced Reactions on ^{6}Li, ^{9}Be, ^{12}C and ^{23}Na Nuclei at Low Energies

M. Yiğit

Published online: 20 September 2014

Abstract In the present work, the excitation functions of neutron reactions ^{6}Li(n,p)^{6}He, ^{9}Be(n,α)^{6}He, ^{12}C(n,p)^{12}B, ^{12}C(n,α)^{9}Be, ^{23}Na(n,p)^{23}Ne, ^{23}Na(n,2n)^{22}Na and ^{23}Na(n,α)^{20}F produced by the incident neutrons were studied for the investigation of fusion structural materials. Tel et al. formulae (for sodium isotopes), the codes ALICE–ASH and CEM03.01 (for all nuclei) were employed for the obtaining of cross-sections. In addition, hybrid model and geometry-dependent hybrid model with pre-equilibrium emissions, and Weisskopf Ewing model with the equilibrium emissions, and the cascade-exciton model with cascade interactions were used to calculate the excitations curves. The obtained results and Tendl-2011 library data were compared with the experimental literature values. Finally it is to mention that the cross-section data obtained may be useful for the safety design of future fusion reactors.

Keywords ALICE–ASH code · Excitation curve · Equilibrium emission · Fusion structural materials

Introduction

Data on the cross-sections for nuclear reactions produced by the particles on different target nuclei are needed in especially fusion and fission reactor applications, radiation damage, medical physics, radionuclide production, dosimetry and other areas [1–3]. Particularly, neutron particles up to excitation energies of 20 MeV have been widely utilised in the research-development related to future fusion technology and fast reactors [4]. Nuclear fusion between many applications is one of attractive long term energy sources [5]. Around the world, fusion materials programs for nuclear energy have very strong emphasis on structural fusion materials research-development [6]. There are many factors that must be considered in selection of the material systems have potential for fusion reactor blanket, first wall, and divertor, structural applications [5]. Furthermore, the plasma facing components, such as divertor, first wall and breeding blanket in the fusion reactors will be exposed to the electromagnetic radiation and the plasma particles, and will thus be suffered from irradiation by an intense fluence of the high energy neutron particles. Indeed, the neutron particles will induce the degradation of series properties of the structural materials and result in residual radioactivity of the materials exposed. Thereby the structural materials of the fusion reactors must show high thermal stress capacity, good compatibility with coolants, high performance and the other materials, high reliability, long lifetime, easy fabrication, reasonable cost, adequate resources, environmental behaviour and good safety. Finally structural materials are one of the key issues for the realization of nuclear fusion energy [7, 8]. The excitation functions of neutron-induced nuclear reactions on sodium (Na) are of great importance because it is known to be a coolant material for fast reactors [9]. Since their behaviour under high heat flux deposition, incident particle bombardment and plasma conditions is very different, the carbon fibre composites and beryllium elements are seriously considered as only a few candidate materials for the plasma facing components [10]. Since Flibe is an excellent attenuator of neutron particles and chemically very stable, BeF_2–2LiF (molten Flibe) is under consideration as a coolant and blanket for the magnetic and inertial fusion

M. Yiğit (✉)
Department of Physics, Faculty of Arts and Science, Aksaray University, Aksaray, Turkey
e-mail: mustafayigit@aksaray.edu.tr

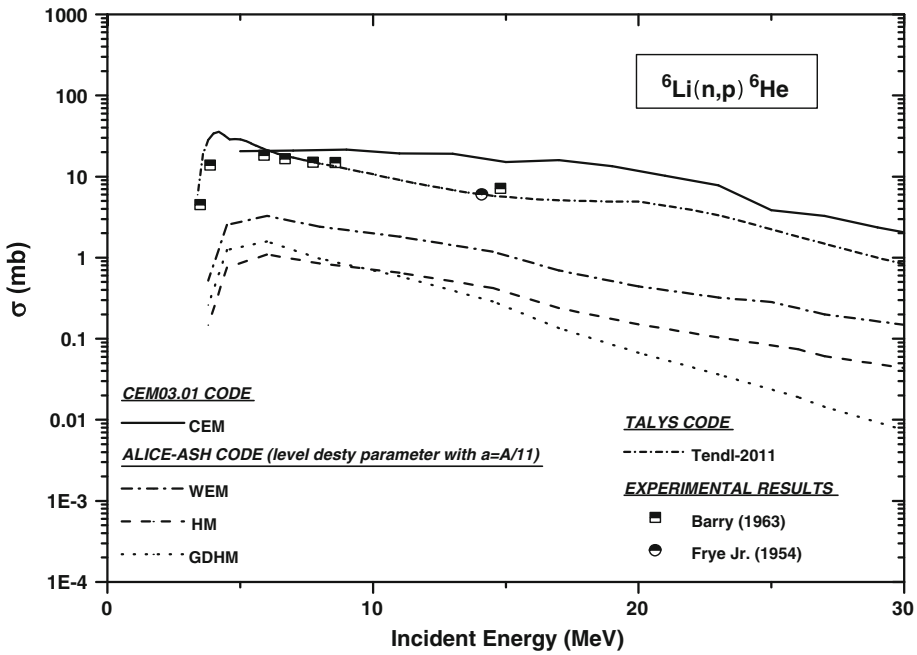

Fig. 1 Cross-sections of ^{6}Li(n,p)^{6}He nuclear reaction calculated by the codes CEM03.01 (CEM), ALICE–ASH (HM, GDHM and WEM), TALYS (Tendl database) and experimental data published by Barry [25] and Frye Jr. [26]

systems [11]. The experimental data for excitation functions of the some nuclear reactions induced by neutron particle are not enough, and also the existing values for other experimental excitation functions are in conflict with each other. Thus, it is needed to use the nuclear model calculations because they give a possibility to predict the excitation functions to energy regions where there are few or no experimental values [9]. Thereby, the model estimations [equilibrium (EQ) and pre-equilibrium (PEQ)] can play an important role to determine the maximum cross-section of (n,x) nuclear reaction. Because of this importance, considerable efforts have thus been devoted to development of nuclear codes. The cross-sections of some nuclear reactions induced on Na nucleus were calculated by the Arasoglu and Ozdemir [12] using the codes CEM95, ALICE–ASH and PCROSS. Moreover, the cross-sections of nuclear reactions induced by neutron particles can be calculated in the framework of the code CEM03.01 [13] and the empirical formulae by Tel et al. In this study, the theoretical results [the empirical formulae by Tel et al., cascade-exciton model (CEM), geometry-dependent hybrid model (GDHM), hybrid model (HM), Weisskopf Ewing model (WEM) and Tendl] of cross-sections of Neutron-Induced nuclear reactions on the structural materials (Lithium, Beryllium, Carbon and Sodium) were presented for neutron energies up to 30 MeV.

Methods for Excitation Function Calculations

Hitherto, a variety of nuclear models and systematics have been used to calculate the cross-sections of the neutron-induced reactions. Tel et al. systematics [14, 15], Tendl-2011 library [16], CEM, equilibrium WEM, pre-equilibrium HM and GDHM have been used to obtain the excitation functions of the (n,x) nuclear reactions. The ALICE–ASH cross-section calculations have been done with nuclear level density parameter a = A/11. The results of the theoretical calculations and experimental data from taken EXFOR [17] were shown in Figs. 1, 2, 3, 4, 5, 6 and 7.

Weisskopf Ewing Model (WEM)

Compound nuclear processes for nuclear reaction dominate in the energy region below 10 MeV. In addition, the equilibrium particle emission is given by the WEM formalism [18] which does not take angular moment conservation into account. The WEM cross-section for incident channel a and exit channel b can be written in the following form,

$$\sigma_{ab}^{WE} = \sigma_{ab}(E_{inc})\Gamma_b \Big/ \sum_{b'} \Gamma_{b'} \quad (1)$$

Here the term E_{inc} denotes incident particle energy. In above formula, the emission probability,

$$\Gamma_b = \frac{2s_b + 1}{\pi^2\hbar^2}\mu_b \int d \in \sigma_b^{inv}(\varepsilon)\varepsilon \frac{\omega_1(U)}{\omega_1(E)} \quad (2)$$

Here the term s_b corresponds to the spin of the outgoing particle from equilibrium nucleus, the term U denotes the excitation energy of residual nucleus, the term μ_b represents the reduced mass of the outgoing particle and the total single-particle level density is taken as below,

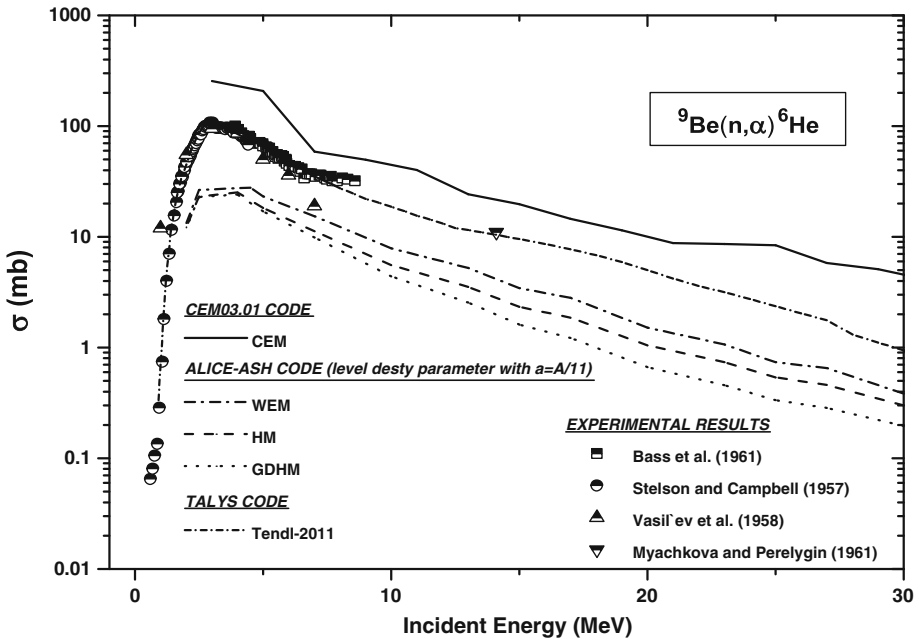

Fig. 2 Cross-sections of ^{9}Be(n,α)^{6}He nuclear reaction calculated by the codes CEM03.01 (CEM), ALICE–ASH (HM, GDHM and WEM), TALYS (Tendl database) and experimental data published by Bass et al. [27], Stelson and Campbell [28], Vasil'ev et al. [29], Myachkova and Perelygin [30]

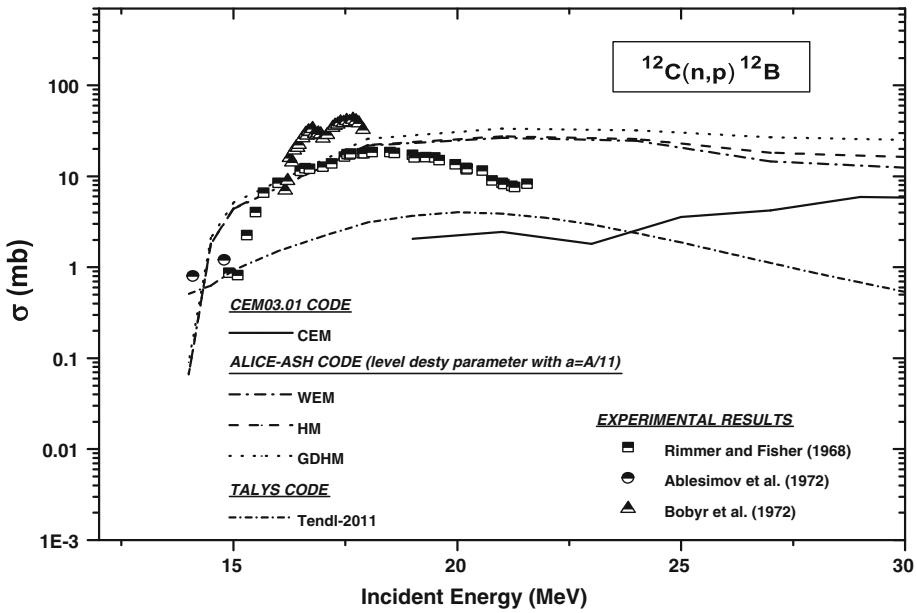

Fig. 3 Cross-sections of ^{12}C(n,p)^{12}B nuclear reaction calculated by the codes CEM03.01 (CEM), ALICE–ASH (HM, GDHM and WEM), TALYS (Tendl database) and experimental data published by Rimmer and Fisher [31], Ablesimov et al. [32] and Bobyr et al. [33]

$$\omega_1(E) = \frac{1}{\sqrt{48}} \frac{exp\left[2\sqrt{\alpha(E-D)}\right]}{E-D}; \quad \alpha = \frac{6}{\pi^2} g \tag{3}$$

Here the term σ_b^{inv} represents the inverse reaction cross-section, the term g is the single-particle level density, the term D is the pairing energy and E is the excitation energy of the equilibrium nucleus [18, 19].

Hybrid Model (HM)

The HM which was first put forward by Blann, describes the pre-equilibrium nuclear reaction mechanism [20, 21].

$$\frac{d\sigma_\upsilon(\varepsilon)}{d\varepsilon} = \sigma_R P_\upsilon(\varepsilon) \tag{4}$$

$$P_\upsilon(\varepsilon)d\varepsilon = \sum_{\substack{n=n_0 \\ \Delta n=+2}}^{\bar{n}} \left[{}_n\chi_\upsilon N_n(\varepsilon, U)/N_n(E)\right] g_\upsilon \, d\varepsilon [\lambda_c(\varepsilon)/(\lambda_c(\varepsilon) + \lambda_+(\varepsilon))] D_n \tag{5}$$

Here, the ${}_n\chi_\upsilon$ denotes the exciton number of ν type nucleon for a given total exciton state n. The term σ_R is the cross-section of the nuclear reaction. Also, the factor $P_\upsilon(\varepsilon)d\varepsilon$ corresponds to the nucleon number of the ν type emitted into the unbound continuum with channel energy between ε

and $\varepsilon + d\varepsilon$. The term $N_n(E)$ denotes the nucleon–nucleon scattering energy partition function, and the term g_v represents the single-particle level density for nucleon of the ν type. In the equal, the term $\lambda_+(\varepsilon)$ is the intra-nuclear transition rate for particles and the term $\lambda_c(\varepsilon)$ for particles with "ε" channel energy represents continuum emission rate. The term D_n is a depletion factor, which corresponds to the average fraction of the initial population surviving to the exciton number being treated. U (residual nucleus excitation energy) is equal to "$E-B_\nu-\varepsilon$". Also the term B_ν corresponds to the binding energy of nucleon of the ν type, and term E represents the excitation energy of composite system [19].

Geometry-Dependent Hybrid Model (GDHM)

The GDHM is a version of the HM, in which the nuclear geometry effects are considering [22]. The differential emission spectrum in the GDHM is calculated in the following form,

$$\frac{d\sigma_\upsilon(\varepsilon)}{d\varepsilon} = \pi \lambda\!\!\!^{-2} \sum_{\ell=0}^{\infty} (2\ell+1) T_\ell P_\upsilon(\ell,\varepsilon) \quad (6)$$

Here the term T_ℓ corresponds to the transmission co-efficient for the ℓth partial wave, and the term $\lambda\!\!\!^{-}$ represents the reduced de-Broglie wavelength of the projectile particle. Also the term $P_\upsilon(\ell, \varepsilon)$ denotes the decay probability at exit channel energy [19, 22].

Cascade Exciton Model (CEM)

The CEM assumes that the reactions consist of stages as intra-nuclear cascade, equilibrium and pre-equilibrium. According to this model, the bombarding particle strikes a nucleon in the target nucleus and then the intra-nuclear cascade stage begins. Generally, these processes may contribute to any measured experimental quantity [23, 24]

$$\sigma(p)dp = \sigma_{in}[N^{cas}(p) + N^{prq}(p) + N^{eq}(p)]dp, \quad (7)$$

In above formula, the term p denotes linear momentum. The term N defines the total particle number and the term σ_{in} is inelastic cross-section calculated by the cascade model [13].

Tendl-2011

Tendl (TALYS-based evaluated nuclear data library) is a nuclear data library that provides the output of the TALYS computer code for direct use in both basic physics and applications with some modifications. The fourth version is Tendl-2011 which is based on both the default and the adjusted TALYS calculations and the data from other sources [16].

(n,p), (n,2n) and (n,α) Empirical Cross-Section Formulae at 14–15 MeV

The empirical formulae include generally the exponential dependence on cross-section of the nucleon number in target nuclei. The systematics and reaction mechanisms the of (n,2n), (n,p) and (n,α) cross-sections of the nuclear reactions produced by neutron particles have been subject of the continuous interest in neutron physics. The (n,2n), (n,p) and (n,α) formulae by the Tel et al. [14, 15] at 14–15 MeV projectile neutron energy have been given as follows (in mb),

$$\ln \sigma_{n,2n} = 7.43[1 - 1.71\exp(-24.99\ s)] \quad (8)$$

$$\sigma_{n,p} = 14.56(A^{1/3}+1)^2 \exp[-26.58s] \quad (9)$$

$$\sigma_{n,\alpha} = 16.15(A^{1/3}+1)^2 \exp[-33.01\ s] \quad (10)$$

Here term s = (N−Z)/A is asymmetry parameter.

Results

^{6}Li(n,p)^{6}He Reaction

The calculated cross-sections (WEM, HM, CEM and GDHM), Tendl-2011 and experimental data for the ^{6}Li(n,p) reaction are plotted in Fig. 1. For ^{6}Li(n,p)^{6}He reaction, TALYS-based Tendl-2011 cross-section data are in good agreement with the existing experimental data reported by Barry [25] and Frye Jr. [26]. Additionally, Tendl data for ^{6}Li(n,p) reaction produced by neutrons shows a maximum of 35.8 mb at about 4.2 MeV. As seen in Fig. 1, the HM, GDHM and WEM estimations with the code ALICE are appreciably lower than the other cross-section values. On the other hand CEM calculations with the code CEM03.01 are higher than equilibrium and pre-equilibrium model calculations with the code ALICE/ASH for considered nuclear reaction.

^{9}Be(n,α)^{6}He Reaction

The theoretical and experimental excitation function curves for ^{9}Be(n,α)^{6}He nuclear reaction are shown in Fig. 2 at the investigated energy region. The code TALYS (Tendl-2011) cross-sections are in good agreement with the results of Bass et al. [27], Stelson and Campbell [28], Vasil'ev et al. [29], Myachkova and Perelygin [30] published in the literature. It appears that the excitation function curves (Tendl and ALICE–ASH) reach the maximum cross-section data at 2.5–4.5 MeV. The ALICE calculations (EQ and PEQ) give lower data than both theoretical (Tendl and CEM) and the experiment results. The CEM with cascade

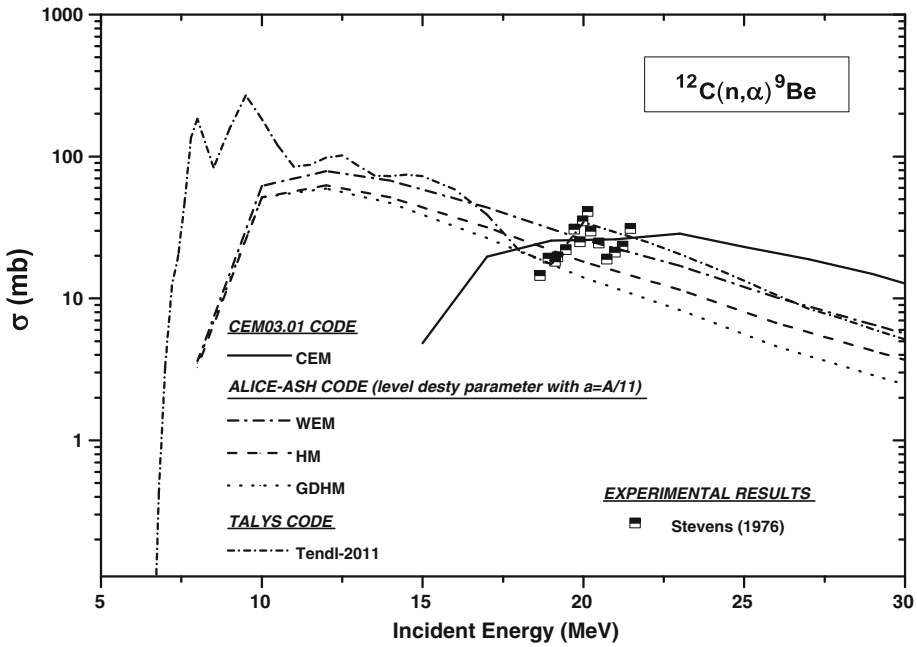

Fig. 4 Cross-sections of $^{12}C(n,\alpha)^{9}Be$ nuclear reaction calculated by the codes CEM03.01 (CEM), ALICE–ASH (HM, GDHM and WEM), TALYS (Tendl database) and experimental data published by Stevens [34]

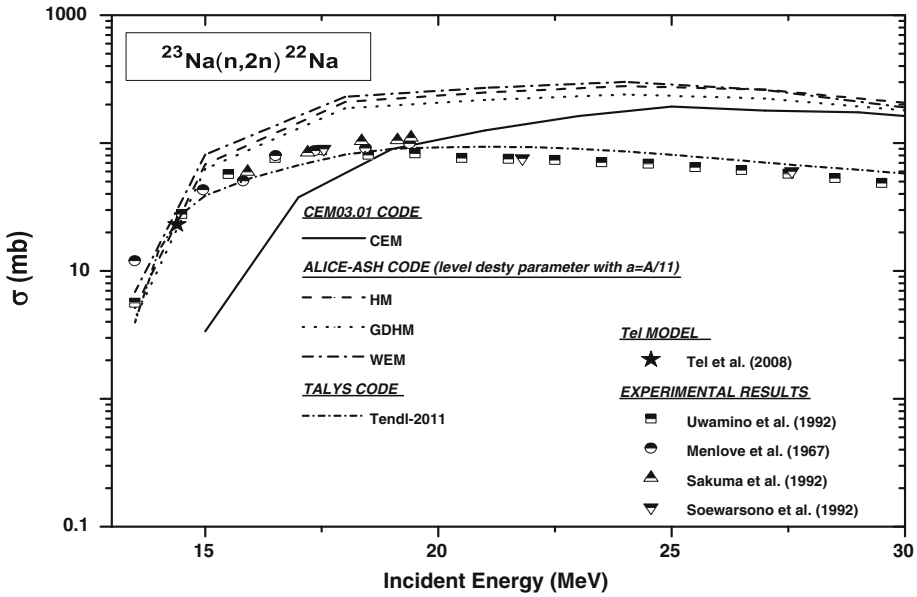

Fig. 5 Cross-sections of $^{23}Na(n,2n)^{22}Na$ nuclear reaction calculated by the codes CEM03.01 (CEM), ALICE–ASH (HM, GDHM and WEM), TALYS (Tendl database), Tel et al. [15] empirical formula and experimental data published by Uwamino et al. [35], Menlove et al. [36], Sakuma et al. [37], and Soewarsono et al. [38]

interactions give higher values than the experimental data the energy range studied.

$^{12}C(n,p)^{12}B$ Reaction

Calculated excitation function curves together with the cross-section data published by Rimmer and Fisher [31], Ablesimov et al. [32] and Bobyr et al. [33] for reaction $^{12}C(n,p)^{12}B$ are presented, as shown in Fig. 3. The considered reaction is energetically possible above 14 MeV. It appears that excitation function results reported by Bobyr et al. [33] have higher values than the other cross-sections. The experimental data of Ablesimov et al. [32], and Rimmer and Fisher [31] give good agreement with ALICE–ASH calculations at low energies. The excitation function result of the CEM calculations with CEM03.01 code is disparate from other cross-section data. Generally Tendl results with the code TALYS are lower than EQ and PEQ model calculations with the code ALICE–ASH.

Table 1 Comparison of the theoretical and experimental cross-sections (in mb) of ^{23}Na(n,p)^{23}Ne, ^{23}Na(n,2n)^{22}Na and ^{23}Na(n,α)^{20}F nuclear reactions at 14–15 MeV projectile energy

Reaction	WEM	HM	GDHM	CEM	Tendl	Tel et al. formulae	Experimental results
^{23}Na(n,2n)	81.17	68.2	62.8	3.37	27.8	23.18	27.84
^{23}Na(n,p)	37.6	46.9	57.7	39.99	45.61	67.73	43
^{23}Na(n,α)	161.2	126.4	108.4	43	112.204	56.8	83.3

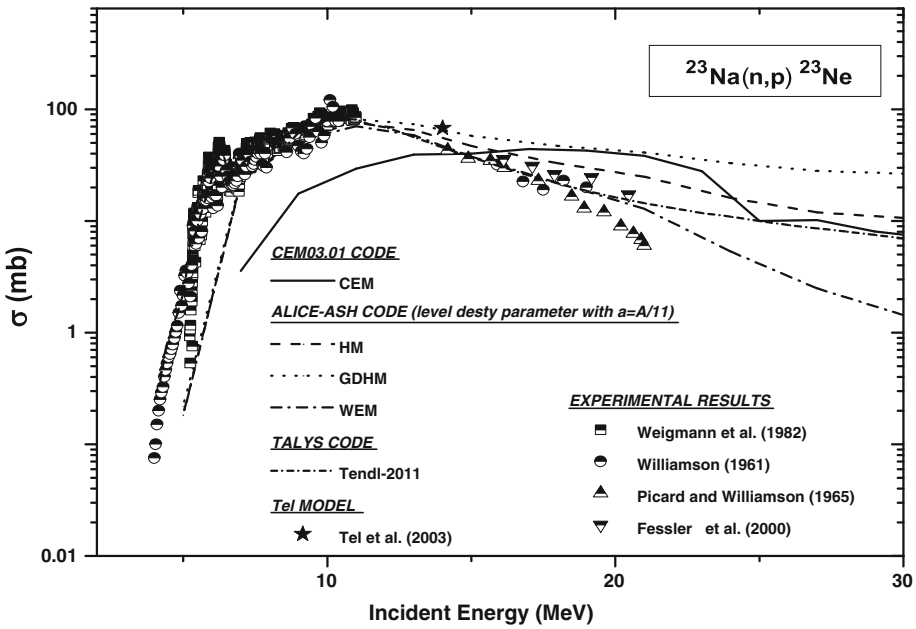

Fig. 6 Cross-sections of ^{23}Na(n,p)^{23}Ne nuclear reaction calculated by the codes CEM03.01 (CEM), ALICE–ASH (HM, GDHM and WEM), TALYS (Tendl database), Tel et al. [14] empirical formula and experimental data published by Weigmann et al. [39], Williamson [40], Picard and Williamson [41], and Fessler et al. [42]

^{12}C(n,α)^{9}Be Reaction

In Fig. 4, the measured data of Stevens [34] together with the results of theoretical calculations are illustrated graphically as a function of the bombarding neutron energy. It seems that the results of theoretical calculation taken from the Tendl database are consistent with the cross-section data reported by Stevens [34]. Also the magnitude of cross-section results of CEM with the CEM03.01 code agrees generally with the measured data of Stevens [34] for the investigated reaction. Cross-section results from the WEM, HM and GDHM with the code ALICE are low values while the Tendl results show generally high data in the studied energy range. The maximum position of excitation curve by the ALICE code (WEM) is 78.8 mb (E_n = 12 MeV).

^{23}Na(n,2n)^{22}Na Reaction

The cross-sections of the ^{23}Na(n,2n)^{22}Na reaction induced by neutrons are shown in Fig. 5 and Table 1. There is a good agreement between the Tendl library and the measured cross-sections presented by Uwamino et al. [35], Menlove et al. [36], Sakuma et al. [37], and Soewarsono et al. [38]. Particularly, the calculated (n,2n) cross-section using the empirical formula by the Tel et al. [15] at 14–15 MeV incident energy for the this reaction gives nearly same results with the measured data of Uwamino et al. [35]. It should be noted the excitation function results calculated by ALICE code (WEM, HM and GDHM) have higher values than the other cross-sections. Additionally the calculated and measured maximum values of excitation curves are not clear for this reaction at the investigated energy region.

^{23}Na(n,p)^{23}Ne Reaction

The experimental data and the theoretical cross-section data for ^{23}Na(n,p)^{23}Ne reaction are presented in Fig. 6 and Table 1. Generally, the Tendl data are in good agreement with the excitation curves reported by the authors Weigmann et al. [39], Williamson [40], Picard and

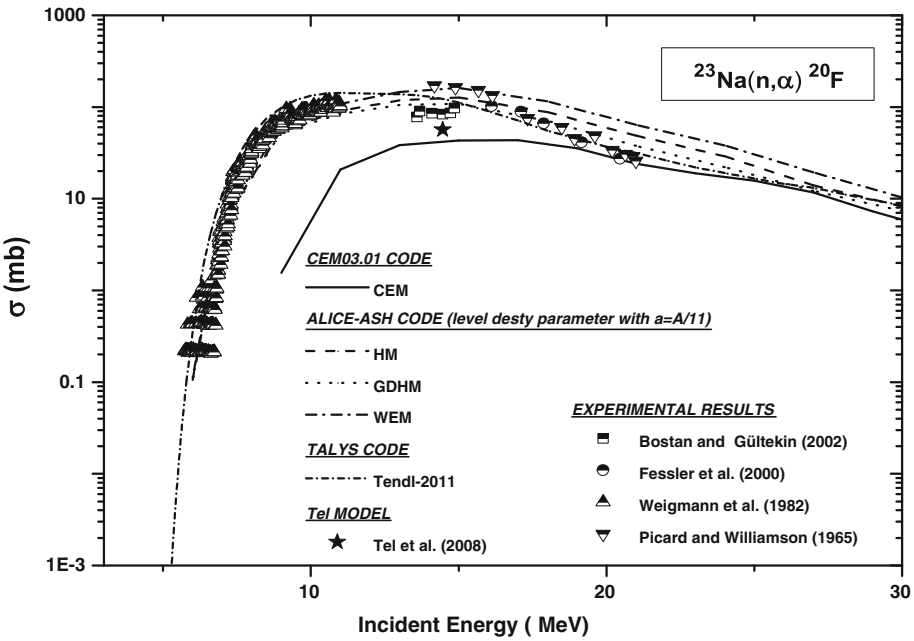

Fig. 7 Cross-sections of ^{23}Na(n,α)^{20}F nuclear reaction calculated by the codes CEM03.01 (CEM), ALICE–ASH (HM, GDHM and WEM), TALYS (Tendl database), Tel et al. [15] empirical formula and experimental data published by Bostan and Gültekin [43], Fessler et al. [42], Weigmann et al. [39], and Picard and Williamson [41]

Williamson [41], and Fessler et al. [42]. The code ALICE–ASH (GDHM) predicted the maximum cross-section to be about 81.7 mb at 11 MeV. It should be noted the CEM cross-section calculation results using the code CEM03.01 gives quite different the structure and magnitude of the excitation curve for the ^{23}Na(n,p)^{23}Ne nuclear reaction. The obtained cross-section value using the empirical formula by the Tel et al. [14] at 14–15 MeV incident neutron energy for the considered (n,p) reaction is in good agreement with the measured data and the model predictions.

^{23}Na(n,α)^{20}F Reaction

Table 1 and Fig. 7 show the theoretical calculations and the experimental results taken from the literature for ^{23}Na(n,α)^{20}F reaction. The ALICE–ASH (WEM, HM and GDHM) and TALYS (Tendl-2011) results are very close with the measured cross-sections published by Bostan and Gültekin [43], Fessler et al. [42], Weigmann et al. [39], and Picard and Williamson [41] for the studied nuclear reaction. Good agreement was found between the CEM and the other calculations in 18–30 MeV energy range. Especially, the calculated cross-section data using the empirical formula by the Tel et al. [15] at 14–15 MeV incident neutron energy for the investigated reaction agrees well with the measured data of Bostan and Gültekin [43] and the CEM results. The theoretically cross-section results for studied (n,α) nuclear reaction appear to give maximum data about incident neutron energy 10–15 MeV. The maximum position of excitation curve by the ALICE code (WEM) is 161.2 mb (E_n = 15 MeV).

Conclusions

Theoretical calculations have been carried out and comparison with experimental literature cross-section data on structural materials was performed. Generally, Tel et al. cross-section systematic results for neutron-induced reactions on Na isotopes give a successful prediction of the experimental literature data. The HM and GDHM give approximately the same results for considered reactions on the structural materials at investigated energy region. Generally, the shape of the excitation functions obtained with the CEM does not follow the trend of the experimental data. The cross-section results of the TALYS code calculations taken from the Tendl-2011 library are in good agreement with the literature measurements except the ^{12}C(n,p)^{12}B nuclear reaction. Here it is to mention that the cross-section data obtained may be useful for the safety design of future fusion reactors.

Acknowledgments The author would like to thank Prof. Eyyup Tel for his guidance during the execution of this work.

References

1. M. Yiğit et al., J. Fusion Energ. **32**, 336–343 (2013)
2. M. Yiğit, E. Tel, J. Fusion Energ. **32**, 442–450 (2013)
3. M. Yiğit, E. Tel, Ann. Nucl. Energ. **69**, 44–50 (2014)
4. S.M. Qaim, J. Radioanal. Nucl. Chem. **284**, 489–505 (2010)
5. E.E. Bloom, J. Nucl. Mater. **7**, 258 (1998)
6. E.E. Bloom et al., J. Nucl. Mater. **329**, 12 (2004)
7. N. Baluc et al., Nucl. Fusion **47**, 696 (2007)
8. Q.Y. Huang et al., J. Nucl. Mater. **386**, 400 (2009)
9. E.L. Trykov, I.R. Svinin, INDC(CCP)-425 (2000)

10. M. Rubel, J. Fusion Sci. Technol. **53**, 459 (2008)
11. M.F. Simpson et al., Fusion Eng. Des. **81**, 541 (2006)
12. A. Arasoglu, O.F. Ozdemir, J. Fusion Energ. (2014). doi:10.1007/s10894-014-9742-1
13. S.G. Mashnik et al., CEM03.01User Manual, Los Alamos National Laboratory Report, LA-UR-05-7321 (2005)
14. E. Tel et al., J. Phys. G. Nucl. Part. Phys. **29**, 2169 (2003)
15. E. Tel et al., Int. J. Mod. Phys. E **17**(3), 567 (2008)
16. A.J. Koning, D. Rochman, TENDL-2011: TALYS-based evaluated nuclear data library. http://www.talys.eu/tendl-2011 (2011)
17. Experimental nuclear reaction data (EXFOR), database version of September 17, 2013, http://www.nndc.bnl.gov/exfor/exfor.htm
18. V.F. Weisskopf, D.H. Ewing, Phys. Rev. **57**, 472 (1940)
19. C.H.M. Broeders et al., ALICE/ASH—pre-compound and evaporation model code system for calculation of excitation functions, energy and angular distributions of emitted particles in nuclear reactions at intermediate energies, FZK 7183, May 2006, http://bibliothek.fzk.de/zb/berichte/FZKA7183.pdf
20. M. Blann, Phys. Rev. Lett. **27**, 337 (1971)
21. M. Blann, H.K. Vonach, Phys. Rev. **C 28**, 1475 (1983)
22. M. Blann, Phys. Rev. Lett. **28**, 757 (1972)
23. S.G. Mashnik, *User manual for the code CEM95* (Joint Institute for Nuclear Research, Dubna, 1995)
24. K.K. Gudima et al., Nucl. Phys. **A 401**, 329 (1983)
25. J.F. Barry, J. Nucl. Energy, Parts A/B React. Sci. Technol. **17**, 273 (1963)
26. G.M. Frye Jr, Phys. Rev. **93**, 1086 (1954)
27. R. Bass et al., Nucl. Phys. **23**, 122 (1961)
28. P.H. Stelson, E.C. Campbell, Phys. Rev. **106**, 1252 (1957)
29. S.S. Vasil'ev et al., Sov. Phys. Dokl. **3**, 354 (1958)
30. S.A. Myachkova, V.P. Perelygin, J. Exptl. Theoret. Phys. **40**, 1244 (1961)
31. E.M. Rimmer, P.S. Fisher, Nucl. Phys. **A108**, 567 (1968)
32. V.E. Ablesimov et al., Conf. Neutron Phys., Kiev, **1,** 173 (1971)
33. V.V. Bobyr et al., Izv. Akad. Nauk SSSR, Ser. Fiz. **36**, 2621 (1972)
34. A. P. Stevens, Report: INIS microfiche No.3596 (1976)
35. Y. Uwamino et al., Nucl. Sci. Eng. **111**, 391 (1992)
36. H.O. Menlove et al., Phys. Rev. **163**, 1308 (1967)
37. M. Sakuma et al., Report: JAERI-M Reports No. 92,027, 278 (1992)
38. T. S. Soewarsono et al., Conf. Rep.: JAERI-M Reports No. 92,027, 354 (1992)
39. H. Weigmann et al., Conf. Nucl. Data Sci. Technol., Antwerp, 814. (1982)
40. C.F. Williamson, Phys. Rev. **122**, 1877 (1961)
41. J. Picard, C.F. Williamson, Nucl. Phys. **63**, 673 (1965)
42. A. Fessler et al., Nucl. Sci. Eng. **134**, 171 (2000)
43. M. Bostan, E. Gültekin, Ann. Nucl. Energy **29**, 2019 (2002)